JPE 7-1-10

Automatic Turn-off Angle Control for High Speed SRM Drives

Maged N. F. Nashed†*, Kazuhiro Ohyama**, Kenichi Aso**, Hiroaki Fujii***, and Hitoshi Uehara***

†*Electronics Research Institute (ERI), Power Electronics & Energy Conversion Dep., Egypt
**Electrical Dep., Fukuoka Institute of Technology, Fukuoka, Japan
***Meiwa Manufacturing Co., Ltd, Fukuoka, Japan

ABSTRACT

This paper presents a new approach to the automatic control of the turn-off angle used to excite the Switched Reluctance Motor (SRM) employed in electric vehicles (EV). The controller selects the turn-off angle that supports and improves the performance of the motor drive system. This control scheme consisting of classical current control and speed control depends on a lookup table to take the best result of the motor. The turn-on angle of the main switches of the inverter is fixed at 0° and the turn-off angle is variable depending on the reference speed. The motor, inverter and control system are modeled in Simulink to demonstrate the operation of the system.

Keywords: Switched Reluctance Motor (SRM), PI Current control, Speed Control, and Turn-off control

1. Introduction

SRM is a motor using reluctance torque which originates from the change of the magnetic resistance in the magnetic circuit. The stator and rotor have a salient pole structure, and they are made from laminated non-oriented electrical steel. The concentrated winding coils are installed only in the stator. SRM has solid features and is characterized by its low cost, since SRM has a structure which has a simpler design than the induction motor and synchronous motor. Also, winding coils and a permanent magnet are not used in the rotor. Therefore, SRM has the possibility of standing high-speed rotations and operations in a high temperature state. SRM is suitable for applications in EV running on roads with inferior conditions and subject to impacts and vibration, [1, 2].

The problems of torque pulsation and noise were big in the initial development of SRM drive. However, those problems are being solved by the development of the power electronics and improvement in the technology [3]. The improvement of basic performance for the SRM drive contributes to the extension of the application field, and the application of SRM to the electric automobile (EV) has begun to be examined recently.

This paper presents an automatic turn-off angle (θ_{off}) control that supports Torque operation of the SRM over its entire speed region. This control depends on the lookup table or equations between reference speed and motor current to select the best turn-off angle. This approach is an alternative to the classic control of speed and the self-tuning approach to optimization of excitation parameters

Manuscript received Feb. 26, 2006; revised Dec. 21, 2006
†Corresponding Author: maged@eri.sci.eg
Tel: +202-3310552, Fax: +202-3351631
Electronics Research Institute (ERI)

[4]. This method is simulated with 600W SRM as a sample machine for comparison.

2. SRM Control

2.1 Current Control

The design of the controllers can be primarily considered when a single phase conducts at a time. It may not be necessary to design for periods of multi-phase conduction. Assuming that phase-a is under consideration, the voltage equation with this converter is written as, [5, 6, 7]

$$\begin{aligned} V_i &= R_S i_a + \frac{d}{dt}(L_a i_a) = R_S i_a + L_a \frac{di_a}{dt} + i_a \frac{dL_a}{dt} \\ &= R_S i_a + L_a \frac{di_a}{dt} + i_a \frac{dL_a}{d\theta}\frac{d\theta}{dt} = R_S i_a + L_a \frac{di_a}{dt} + i_a \omega_m \frac{dL_a}{d\theta} \\ &= i_a(R_S + \omega_m g_L) + L_a \frac{di_a}{dt} \end{aligned} \quad (1)$$

Where the rate of change of inductance is constant and defining,

$$g_L = i_a \omega_m \frac{dL_a}{d\theta} \quad (2)$$

The electromagnetic torque can be calculated as,

$$T_e = \frac{1}{2} g_L i_a^2 \quad (3)$$

Assuming that the load is proportional to the speed, at rated speed and rated load torque,

$$B_\ell = \frac{T_e^{rat}}{\omega_m} \quad (4)$$

The total inertia of the machine can be calculated as,

$$B_t = B + B_\ell$$

The mechanical equation can be written as,

$$\begin{aligned} T_e &= J\frac{d\omega_m}{dt} + B_t \omega_m \\ \frac{1}{2} g_L i_a^2 &= J\frac{d\omega_m}{dt} + B_t \omega_m \end{aligned} \quad (5)$$

Equations (1) and (5) represent the machine equations. Since (5) is nonlinear, the equation can be linearized and the small signal equations can be used for analysis. Therefore,

$$V_{io} + \delta V_i = (i_{ao} + \delta i_a)(R_S + (\omega_{mo} + \delta\omega_m) g_L) + L_a \frac{d(i_a + \delta i_a)}{dt} \quad (6)$$

$$\frac{1}{2} g_L (i_{ao} + \delta i_a)^2 = J\frac{d(\omega_{mo} + \delta\omega_m)}{dt} + B_t(\omega_{mo} + \delta\omega_m) \quad (7)$$

Neglect $\delta i_a \delta\omega_m g_L$ and $(\delta i_a)^2$

The small signal equations are given by,

$$\delta V_i = \delta i_a (R_S + \omega_{mo} g_L) + L_a \frac{d(\delta i_a)}{dt} + i_{ao} g_L (\delta\omega_m) \quad (8)$$

$$i_{ao} g_L \delta i_a = J\frac{d(\delta\omega_m)}{dt} + B_t(\delta\omega_m) \quad (9)$$

In terms of state space equations, the above equations can be written as,

$$\begin{bmatrix} \frac{d(\delta i_a)}{dt} \\ \frac{d(\delta\omega_m)}{dt} \end{bmatrix} = \begin{bmatrix} \frac{(R_s + \omega_{mo} g_L)}{L_a} & \frac{i_{ao} g_L}{L_a} \\ \frac{i_{ao} g_L}{J} & \frac{B_t}{J} \end{bmatrix} \begin{bmatrix} \delta i_a \\ \delta\omega_m \end{bmatrix} + \begin{bmatrix} \frac{1}{L_a} \\ 0 \end{bmatrix} [\delta V_i] = AX + BU \quad (10)$$

If either A or B contains a function of X or U, it is a nonlinear system. For the case of a linear system, the DC solution is obtained by setting equation (10) to zero to yield

$$X = -A^{-1}BU \quad (11)$$

where A^{-1} is the inverse of the state coefficient matrix. The inverse of a matrix is the adjoint divided by its determinant. Note that the determinant of A must be nonzero for a valid DC solution. Taking the Laplace transform of equation (10)

$$sX(s) = AX(s) + BU(s)$$

or

$$X(s) = (sI - A)^{-1} BU(s) \quad (12)$$

where I is the identity matrix having the same dimension as A. For our simple second-order example, we have

$$\begin{bmatrix} \delta i_a \\ \delta\omega_m \end{bmatrix} = \frac{\begin{bmatrix} S + \frac{B_t}{J} & -\frac{i_{ao} g_L}{L_a} \\ \frac{i_{ao} g_L}{J} & S + \frac{R_s + \omega_{mo} g_L}{L_a} \end{bmatrix} \begin{bmatrix} \frac{1}{L_a} \\ 0 \end{bmatrix} [\delta V_i]}{S^2 + S\left(\frac{B_t}{J} + \frac{R_s + \omega_{mo} g_L}{L_a}\right) + \frac{B_t(R_s + \omega_{mo} g_L) + i_{ao}^2 g_L^2}{L_a J}} \quad (13)$$

To calculate the current loop transfer function and its response, it is necessary to calculate the transfer function,

$$\frac{\delta i_a(S)}{\delta V_i(S)}=\frac{\frac{1}{L_a}(S+\frac{B_t}{J})}{S^2+S\left(\frac{B_t}{J}+\frac{R_s+\omega_{mo}g_L}{L_a}\right)+\frac{B_t(R_s+\omega_{mo}g_L)+i_{ao}^2g_L^2}{L_aJ}}=\frac{(SJ+B_t)}{S^2L_aJ+S(L_aB_t+R_sJ+\omega_{mo}g_LJ)+B_tR_s+\omega_{mo}g_LB_t+i_{ao}^2g_L^2} \quad (14)$$

Defining the mechanical time constant of the machine and the electrical time constant of the machine respectively as,

$$T_m=\frac{J}{B_t} \qquad \tau=\frac{L_a}{R_s} \quad (15)$$

$$\frac{\delta i_a(S)}{\delta V_i(S)}=\frac{B_t(ST_m+1)}{L_aJ\left(S^2+S\left(\frac{1}{T_m}+\frac{1}{\tau}+\frac{\omega_{mo}g_L}{L_a}\right)+\frac{1}{T_m\tau}+\frac{\omega_{mo}g_L}{T_mL_a}+\frac{i_{ao}^2g_L^2}{L_aJ}\right)}=\frac{B_t(ST_m+1)}{L_aJ(S^2+Sb+c)}=\frac{(ST_m+1)}{L_aT_m(S+T_1)(S+T_2)} \quad (16)$$

Where

$$b=\frac{1}{T_m}+\frac{1}{\tau}+\frac{\omega_{mo}g_L}{L_a} \qquad c=\frac{1}{T_m\tau}+\frac{\omega_{mo}g_L}{T_mL_a}+\frac{i_{ao}^2g_L^2}{L_aJ}$$
$$-T_1=\frac{-b-\sqrt{b^2-ac}}{2} \qquad -T_2=\frac{-b+\sqrt{b^2-ac}}{2} \quad (17)$$

The current control loop is shown in Fig. 1. The transfer function of the pulse width modulator is obtained as,

$$G_{PWM}(S)=\frac{d(s)}{V_i(S)}=\frac{K_{PWM}}{1+ST_{PWM}} \quad (18)$$

Where the gain K_{PWM} is given by $K_{PWM}=\frac{V_i}{V_{ramp_{max}}-V_{ramp_{min}}}$, the delay T_{PWM} is given by $T_{PWM}=\frac{1}{2f_C}$, the mechanical time constant T_m is given by $T_m=\frac{J}{B_t}$ T_1 and T_2 are constant and depend on the parameters of the motor.

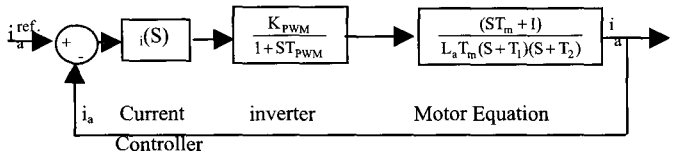

Fig. 1 Current control loop.

The current loop system is simplified as,

$$G_{ic}(S)=\frac{\frac{SK_iK_{PWM}}{L_a}}{S^2+S\left((T_1+T_2)+\frac{K_iK_{PWM}}{L_a}\right)+T_1T_2} \quad (19)$$

2.2 Speed Control with turn-off control

The objectives of the Lookup table calculation are best explained through consideration of the nonlinear inductance for the SRM. The minimum inductance region is defined by the angular interval over which the rotor

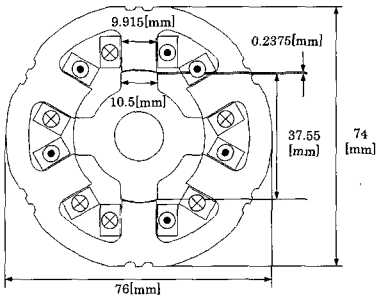

Fig. 2 Analytical model.

TABLE 1 Condition of Analysis

Number of node	15173
Number of element	7636
Mesh size	0.0013
Shape of element	triangle
Excitation phase of coil	one phase only
Magnetomotive force	80 [AT]
Current density	$1.559*10^6$[A/m^2]
Partial area of coil	51.3 [mm^2]
Analysis range	0-45 [deg]

TABLE 2 Specification of SRM

Parameters	Value
Number of stator/ rotor Poles	6/4
Maximum Speed	18000 rpm
DC voltage	24 Volts
Excitation Current	2-30 Amps
Rated Torque	0.1 Nm
Aligned Phase Inductance	2.121 mH
Unaligned Phase Inductance	0.2167 mH
Stator outer diameter	76 mm
Rotor outer diameter	37.55 mm
Air gap	0.2375 mm
Stack length	50 mm
Number of windings/poles	20 turns/poles

poles do not overlap the stator poles. The maximum inductance region is defined by the angular interval over which there is complete overlap between the stator and rotor poles. The regions of increasing and decreasing inductance correspond to varying overlap between the stator and rotor poles.

We have modeled our experimental SRM drive to support simulation studies, details of the motor specification are given in Table 1. The SRM magnetic field has been modeled through finite element analysis to capture the relevant spatial and magnetic nonlinearities that must be considered for meaningful control design, [8, 9].

Inductance and static torque of 600W SRM sample machine are calculated using ANSYS software of FEM. Fig. 2 shows the analytical model of SRM. Table 1 shows the condition of analysis. Table 2 shows the specification of SRM. Using the analytical model as shown in fig. 2, the calculation is carried out by the two-dimensional static magnetic field analysis.

In this analysis, a three-phase SRM which has 6 poles stator and 4 poles rotor of SRM is employed. Since the pole number of the rotor is 4, the magnetic circuit becomes the same after rotating 90 degrees, when only one phase is excited. In addition, the stator salient pole and rotor salient pole repeat facing conditions and non-facing conditions for the interval of rotation 45 degrees. It is possible to obtain the inductance of 360 degree rotation by using the calculated inductance of the 45 degree rotations, if such geometric symmetry is utilized. The non-facing condition of the stator salient pole and rotor salient pole is defined as 0 degrees, and the rotor is made to rotate 45 degrees of the facing condition. For each 1 degree, the inductance and static torque of one phase are calculated.

At rotor position θ, the magnetic co energy W'(θ) is calculated according to the following equation, while the rotor is made to rotate from 0 degrees to 45 degrees for each 1 degree.

$$W'(\theta)=\frac{1}{2}\sum_{i}\frac{B_i^2}{\mu_i}v_i \tag{20}$$

Where B_i is the magnetic flux density of each element, μ_i is the permeability of each element, and v_i is the volume of each element.

Inductance L(θ) in rotor position θ is calculated according to the following equation.

$$L(\theta)=\frac{2W'(\theta)}{i^2} \tag{21}$$

where i is the excitation current.

Fig. 3 shows the inductance L(θ) in rotor position θ calculated using equations (20) and (21) at different values of the stator current.

Using the W'(θ) or L(θ), the reluctance torque T(θ) is calculated according to equation (2).

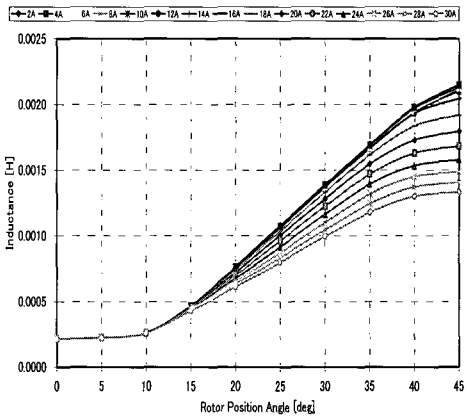

Fig. 3 Linear inductance of the SRM.

Fig. 4 shows static torque T(θ) in rotor position θ calculated using equation (22) at different values of the stator current. T(θ) of the positive direction is obtained regardless of the current direction, if the exciting current is flowing when L(θ) increases, because T(θ) is proportional to the derivative for the rotor position of the inductance. In short, the rotor keeps rotating in the positive direction, because the torque of the positive direction is obtained at every excitation, when the winding continues to be excited in the position where the gradient of L(θ) changes in a positive direction. While Fig. 5 shows the relationship between the stator current and flux interlinkage at different values of the rotor position angle.

The static torque exciting only one phase was measured using a 600W SRM sample machine. Fig. 6 shows the experimental circuit. The excitation current of 4 A is applied to one phase of SRM using the DC power source, and static torque at rotor position θ was measured using the torque meter. The rotor position of SRM was fixed using the brushless DC motor drive. The rotor position of

SRM can be fixed by controlling the rotor position of the brushless DC motor using the brushless DC motor drive. There is a speed reducer between the brushless DC motor and SRM.

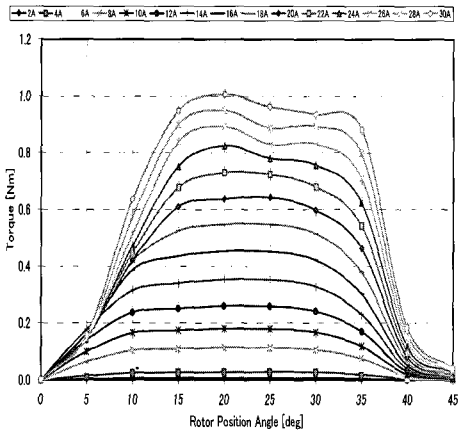

Fig. 4 Relationship between rotor position angle and torque.

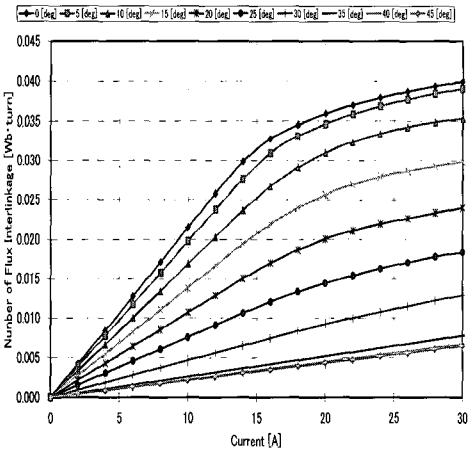

Fig. 5 Relationship between the stator current and flux interlinkage

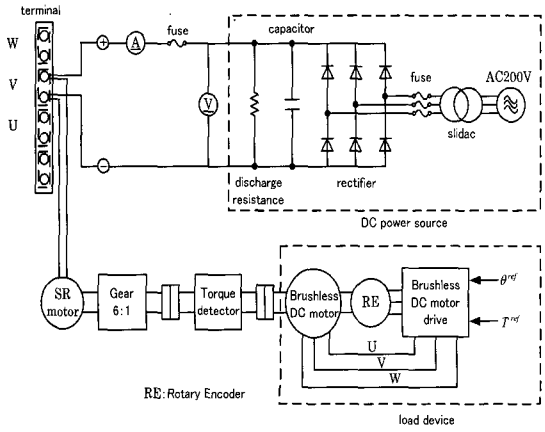

Fig. 6 Experiment circuit.

The gear ratio is 6:1. Therefore, it is possible to rotate the SRM for 1 degree by giving the command signal which rotates 1/6 of a degree to the brushless DC motor drive. Additionally, the static torque in the position fixed by the brushless DC motor drive can be measured using the torque meter. The comparison of calculated and experimental results of the static torque is shown in fig. 7. The static torque calculated using magnetic field analysis agrees well with the experimental result measured under the same condition. Therefore, the validity of the magnetic field analysis using FEM utilized for the design was proven.

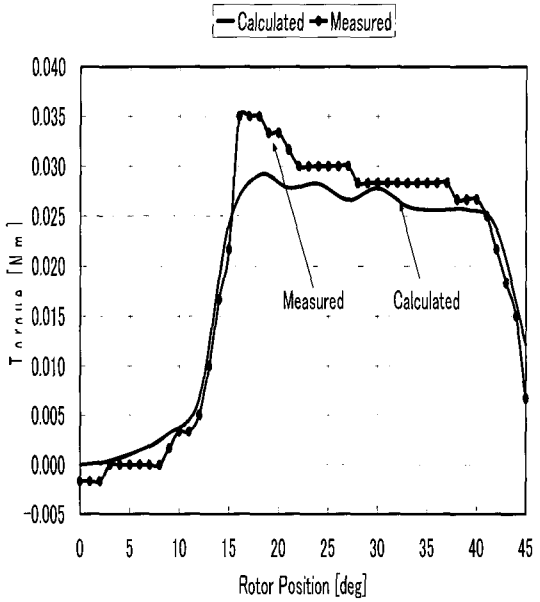

Fig. 7 Comparison of calculated and experimental results of Static torque.

The turn-on angle is advanced or retarded automatically according to the minimum value of inductance. In this control, the SRM is simulated at constant turn-on value 0°, different θ_{off} and different stator current to take the motor speed. We found the relation between speed and θ_{off} at different values of the current. This relation is shown in Fig. 8. All these relations are used in the simulation and control of the motor. We can change the lookup table to the equation for different currents. For example: change the curve at stator current 16 Amps to an equation by polynomial method as:

$$\theta_{off} = -14.01094 + 0.00791\omega - 7.5154E\text{-}7\omega^2 + 2.5801E\text{-}11\omega^3 \quad (22)$$

The control of θ_{off} is summarized in Fig. 9. Fig. 10 shows the operation of the automatic controller for the current control operation of SRM with a change to the reference current from 8Amp to 10Amp at 2.5 sec. At this point in the operation, the speed changes from 5400 to 8600 rpm. While Fig. 11 shows the operation of the automatic controller for θ_{off} control for the operation of SRM with changes to the θ_{off} from 25° to 35° at 2.5 sec. The control of θ_{off} occurs at the same reference current control. The time of speed change is lower than the other control and the speed is the same in two methods. Fig. 12 shows the phase voltage (A) at a change of reference current control with θ_{off} constant while (B) at a change of θ_{off} control with constant reference current. The new control technique provides performance motor operation with ease without the need of the load conditions. In the future, the new control technique will be applied to an experimental system. Fig. 13 shows the rotor speed, stator current and Turn off angle when the reference rotor speed changes from 4000 to 6500 rpm at 5 Sec. While Fig. 14 shows the rotor speed, stator current and Turn off angle when the load torque changes from 0.05[Nm] to 0.10[Nm] at 5 sec.

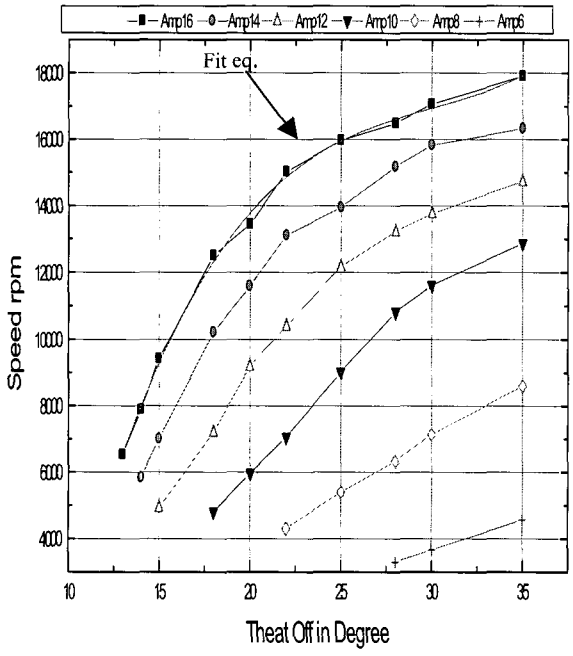

Fig. 8 Relationship between the Turn off angle θ_{off} and speed motor.

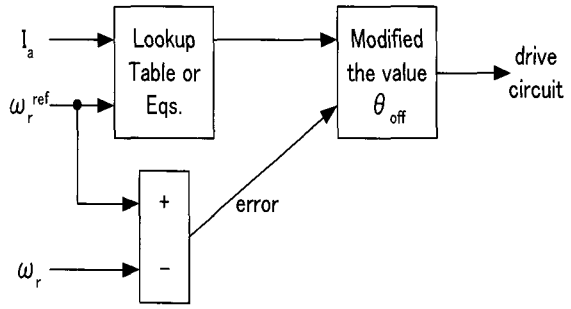

Fig. 9 the Lookup table used to automatically adjust the turn-off angle.

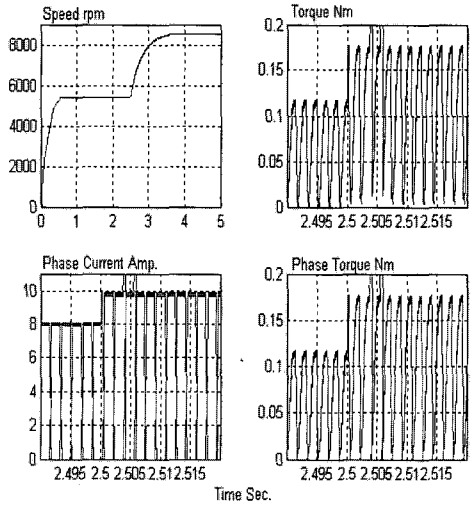

Fig. 10 Simulation System for the current control for SRM With change the reference current from 8 Amp. to 10Amp. at 2.5 sec.

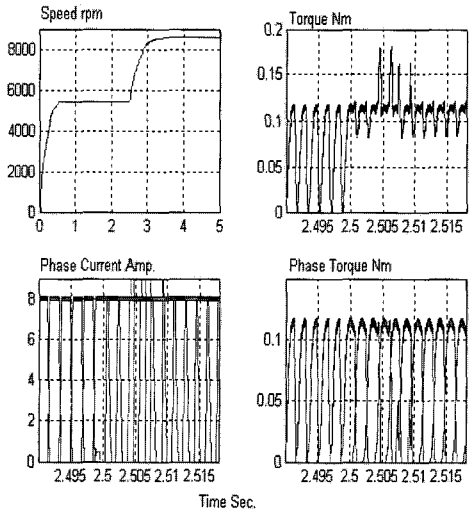

Fig. 11 Simulation system θ_{off} control for SRM with change the θ_{off} from 25° to 35° at 2.5 sec.

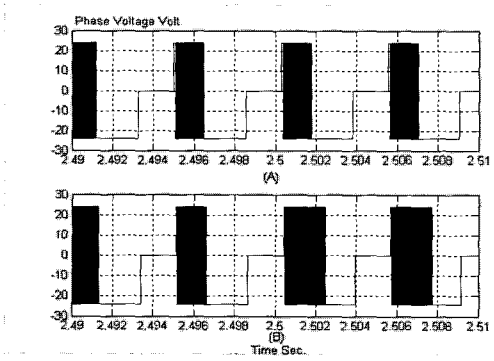

Fig. 12 The Phase voltage (A) at change of reference current control with θ_{off} constant (B) at change of θ_{off} control with constant reference current.

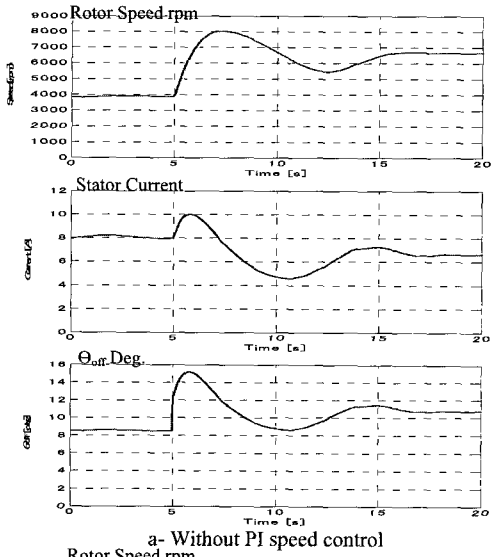

a- Without PI speed control

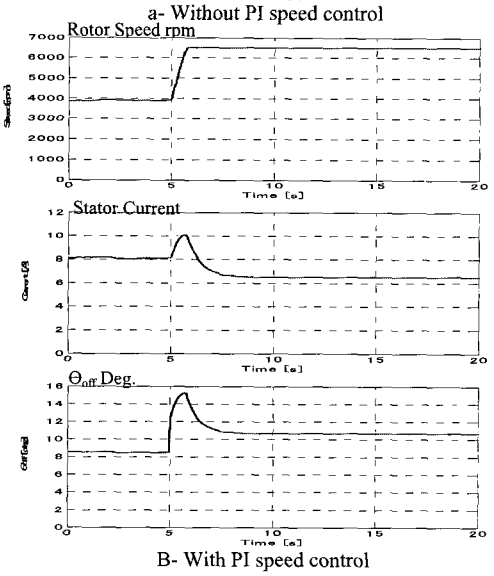

B- With PI speed control

Fig. 13 The simulation result of rotor speed, stator current and Turn off angle with change of reference rotor speed from 4000 to 6500 rpm at 5 Sec.

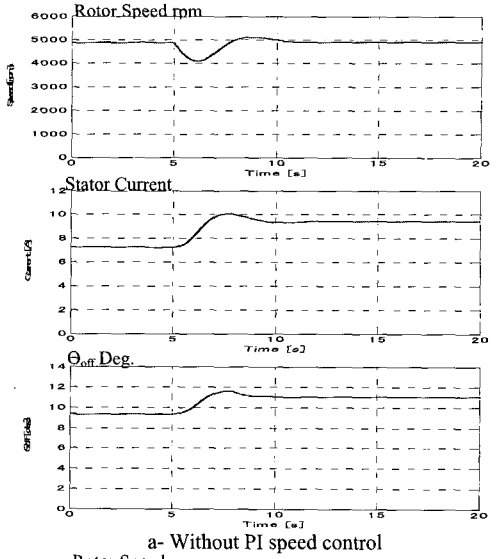

a- Without PI speed control

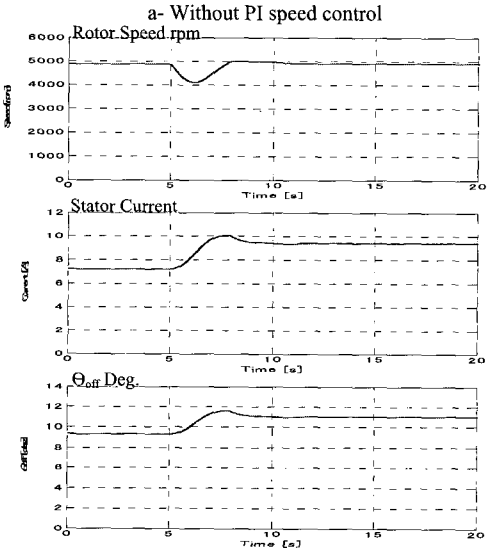

B- With PI speed control

Fig. 14 The simulation result of rotor speed, stator Current and Turn off angle with change of load torque from

3. Conclusions

A new method for the automatic control of θ_{off} has been proposed. This method improved the performance of PI classical control for the SRM. The new approach provides for automatic turn-off angle adjustment without information of the load conditions. . The peak phase current of the stator does not change with the speed variation. The new control method provides positive performance motor operation easily. It was confirmed that the static torque calculated in the magnetic field analysis agreed ideally with the experimental results. Therefore, it

was confirmed that magnetic field analysis using FEM could be utilized for the design of SRM. The motor, inverter and control system are modeled in Simulink to demonstrate the operation of the system

References

[1] A. Chiba, "Design of a Switched Reluctance Drive and Its Application," J. Magn. Soc. Japan, Vol.26, No.8, 909-914, 2002.

[2] K. N. Srinivas, and R. Arumugam, "Dynamic Characterization of Switched Reluctance Motor By Computer-Aided Design and Electromagnetic Transient Simulation" IEEE Transactions on Magnetics, Vol. 39, No. 3, May 2003, pp 1806-1812.

[3] M. Morimoto, N. Matsui, and Y. Takeda, "Recent Advances of Reluctance Motors", IEEJ Trans. IA, Vol.119, No.10, 1145-1148, 1999

[4] K. Russa, I. Husain, and M. Elbuluk, "A self-tuning controller for Switched reluctance motor," IEEE Trans. Power Electronic, Vol.15,pp 545-552, 2000.

[5] S. E. Schulz and K. M. Rahman, "High-Performance Digital PI Current Regulator for EV Switched Reluctance Motor Drives," IEEE Trans. Ind. Applicat., vol. 39, 1118-1126, 2003.

[6] H. C. Lovatt, and J. M. Stephenson "Computer-Optimized Smooth-Torque Current Waveforms for Switched-Reluctance Motors", IEE Proc. Inst. of Elec. Eng., Pt. B, Vol. 144, No. 5, September 1997, pp 310-316.

[7] K. N. Srinivas, and R. Arumugam, "Analysis and Characterization of Switched Reluctance Motor: Part I-Dynamic, Static, and Frequency Spectrum Analyses" IEEE Transactions on Magnetics, Vol. 41, No. 4, April 2005, pp 1306-1320.

[8] K. N. Srinivas, and R. Arumugam, "Finite Element Analysis Combined Circuit Simulation of Dynamic Performances of Switched Reluctance Motor" Int. J. Elect. Power Computer System, Vol. 30, No. 10, October 2002, pp 1033-1045.

[9] K. Ohyama, M. N. F. Nashed, K. Aso, H. Fujii, and H. Uehara "Design Using Finite Element Analysis of Switched Reluctance Motor for Electric Vehicle" Asian Electric Vehicle Conf.-4, Nov. 26-28, Osaka, Japan, 2005.

Maged Naguib Fahmy Nashed received his B.S. degree in Electrical Engineering, from Menoufia University, Egypt, in May 1983, his Diploma of Higher Studies from Cairo University, May 1990, his M.SC. degree in Electrical Engineering, from Ain Shams University, Cairo, Egypt, in April 1995 and his Ph.D. in Electrical Engineering, from Ain Shams University, Cairo, Egypt, in January 2001. He was a researcher for Fukuoka Institute of Technology, Japan, 2005. Since 1989, he has been a researcher with the Department of Power Electronic and Energy Conversion, Electronic Research Institute. He is engaged in research on power electronics, drive circuit, control of drives and renewable energy.

Kazuhiro Ohyama received his B.Eng. degree in Electrical Engineering, M. Eng. and D. Eng. from Kagoshima University, Kagoshima, Japan, in 1993, 1995 and 1998, respectively. He was a visiting scholar at the University of Nottingham, U.K., from 1998 to 1999. In April 1999, he joined the Department of Electrical Engineering, Fukuoka Institute of Technology, as a lecturer. In April 2002, he was promoted to assistant professor. He is currently engaged in the study of motor drives. He is a member of the Institute of Electrical Engineering of Japan.

Kenichi Aso received his B. Eng. degree in Electrical Engineering and M. Eng. from Fukuoka Institute of Technology, Fukuoka, Japan, in 2004 and 2006, respectively. He is currently engaged in the study of switched reluctance motor drives. He is a member of the Institute of Electrical Engineering of Japan.

Hiroaki Fujii received his B. Eng. degree in Electrical Engineering from Fukuoka Institute of Technology, Fukuoka, Japan, in 1981. He is currently engaged in the study of switched reluctance motor design.

Hitoshi Uehara received his B. Eng. degree in Electrical Engineering from Fukuoka Institute of Technology, Fukuoka.